Volume 15
Number 31
21 August 2024
Pages 3115-3216

Polymer Chemistry

rsc.li/polymers

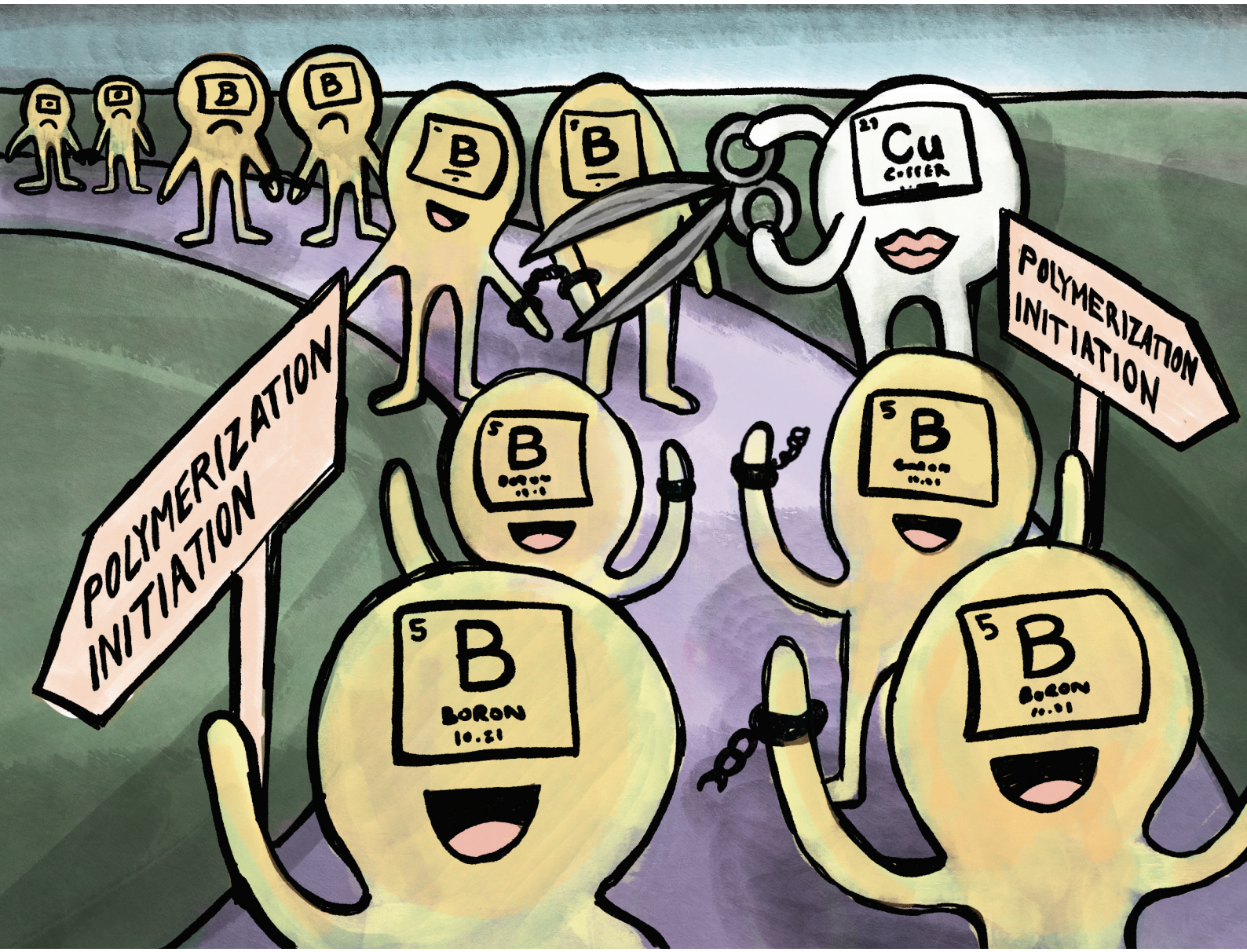

ISSN 1759-9962

ROYAL SOCIETY OF CHEMISTRY

PAPER
Patrick Knaack *et al.*
Boron–boron bonds: boldly breaking boundaries towards amine- and peroxide-free 2K radical polymerization

Polymer Chemistry

ROYAL SOCIETY OF CHEMISTRY

PAPER

View Article Online
View Journal | View Issue

Cite this: *Polym. Chem.*, 2024, **15**, 3127

Boron–boron bonds: boldly breaking boundaries towards amine- and peroxide-free 2K radical polymerization†

Florian Pieringer, [a] Konstantin Knaipp, [b] Robert Liska, [a] Norbert Moszner,[c] Yohann Catel,[c] Georg Gescheidt [b] and Patrick Knaack *[a]

Received 22nd April 2024,
Accepted 6th June 2024

DOI: 10.1039/d4py00445k

rsc.li/polymers

Free radical polymerization (FRP) is one of the most important tools for the production of polymer materials. Many applications of such materials require a convenient polymerization process at room temperature and ambient atmosphere, which is where two-component (2K) systems based on redox initiated radical polymerization truly stand out. However, these radical polymerization systems (RPSs) often require toxic amines and thermally labile (explosive) peroxides as redox pairs. In order to surpass these hazardous limitations, a new RPS for 2K polymerization of industrially implemented methacrylic monomers was developed. The use of diboranes as labile bonds and copper complexes that catalyze their cleavage was found to be a very efficient radical initiation system. High reactivity towards radical polymerization is presented by different combinations of these compounds, and the influence of steric and electrochemical effects is investigated in this context. Furthermore, thermomechanical and mechanical testing of polymer materials was conducted. The obtained polymer networks were found to possess a highly homogeneous structure and furthermore properties that are strongly influenced by the RPS, including the possibility of thermal post-curing reaching T_g's > 150 °C.

Introduction

Polymers have revolutionized multiple industries including packaging, dental restoratives, coatings and adhesives.[1–3] The curing process to obtain the polymer materials is often very energy consuming (*e.g.* thermal curing) and advancements in more energy efficient polymerization processes have been made (*e.g.* photopolymerization, redox polymerization).[1] Recently, photocuring of less hazardous monomers, such as methacrylates, has introduced new possibilities regarding curing speed and toxicity.[4] However, a significant drawback of photopolymerization is a limitation in the depth of curing of bulk materials.[5,6] For applications in bulk curing, two-component (2K) systems are growing steadily as a reliable method for curing at room temperature and under atmospheric conditions.[1,7,8] Furthermore, the necessary energy for such systems to start polymerization is minor compared to other industrially used polymerization methods *e.g.* thermal curing.[1] These 2K systems are often based on a redox pair that initiates the polymerization *via* a redox reaction upon mixing two formulations. Herein, an oxidizing agent is stored in one part of the monomer formulation and a reducing agent is stored in a separate part of the monomer formulation. Currently, the use of thermally labile peroxides as oxidizing agents and toxic amines as reducing agents is highly prevalent in industry.[9–12] In this regard, the combination benzoylperoxide/tertiary aromatic amine is widely applied.[11,12] In addition, amines yield discolored oxidation products, making them unsuitable for applications that require colorstable materials.[13] Recently, new hydroperoxide-based initiation systems are developed in combination with alternative reducing agents such as thioureas, barbituric acid derivatives, ascorbic acid derivatives and sulfonates.[2,14–19] Despite efforts to forgo the use of such hazardous compounds in the radical polymerization system (RPS), only a limited number of alternatives have been reported.[20] Silanes such as diphenyl silane in combination with iodonium salts can be used for 2K polymerization of methacrylic resins and have proven to yield tack-free polymers in combination with phosphines.[21] Furthermore, literature reports the use of different metal acetylacetonates (Cu, Mn, V, ⋯) with bidentate ligands to undergo a ligand exchange reaction leading to the formation of radicals, however, high concentrations (>1 w%) of

[a]*Institute of Applied Synthetic Chemistry, TU Wien, 1060 Vienna, Austria. E-mail: patrick.knaack@tuwien.ac.at*
[b]*Institute of Physical and Theoretical Chemistry, Graz University of Technology, Stremayrgasse 9, 8010 Graz, Austria.*
[c]*Ivoclar AG, Bendererstrasse 2, Schaan 9494, Principality of Liechtenstein*
† Electronic supplementary information (ESI) available. See DOI: https://doi.org/10.1039/d4py00445k

the metal salt are necessary.[22,23] A very neglected class of molecules in this context are diboranes (*e.g.* B_2pin_2). They are widely used in organic synthesis for borylation reactions or as reducing agents.[24–26] To this end, the boron–boron bond is efficiently activated by different Cu compounds (*e.g.* CuCl, Cu(ac)) to yield adducts with α,β-unsaturated carbonyl compounds.[24,26–30] In many cases, it is reported that a radical mechanism is involved during this activation step.[31–33] However, to the best of our knowledge, the use of diboranes in conjunction with Cu salts as activation catalysts has not yet been reported as a radical initiation system for polymerization reactions (Fig. 1).

Herein, we present three diboranes bearing six-membered rings (B6-1, B6-2, B6-3, Scheme 1) with increasing steric demand in proximity to the boron–boron bond. Furthermore, we also investigated diborane species with five-membered rings including B_2pin_2 (here B5-1), asymmetric diboranes (B5-2) and a silyl borane (B5-3, Suginome's reagent). Cu compounds with acetate (Cu(I)ac, Cu(II)ac_2), acetylacetonate (Cu(II)$acac_2$) and tri/hexa-fluorinated acetylacetonate (Cu(II)$tfacac_2$, Cu(II)$hfacac)_2$ ligands were investigated as catalysts for the activation of the aforementioned diborane compounds. The polymerization experiments were carried out in a mixture of

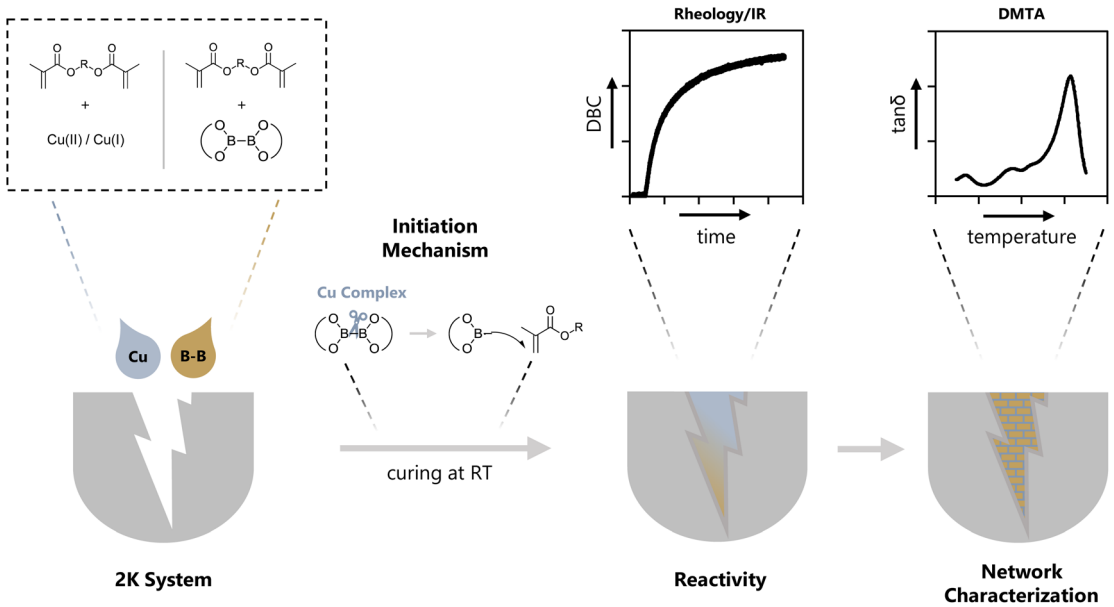

Fig. 1 A newly developed 2K radical initiation system was developed using diboranes and copper catalysts for the polymerization of difunctional methacrylates. In this work, details about the initiation mechanism are presented as well as an investigation of the reactivity towards polymerization depending on the diborane and copper compound used. The yielded polymer networks were investigated regarding their thermomechanical- and mechanical properties.

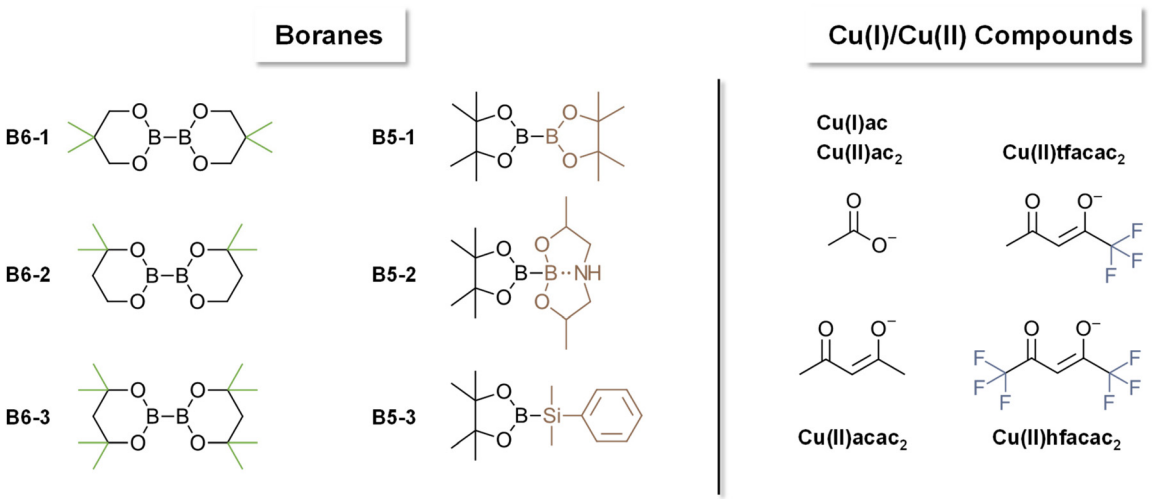

Scheme 1 Chemical compounds studied in this work as initiators for free radical polymerization.

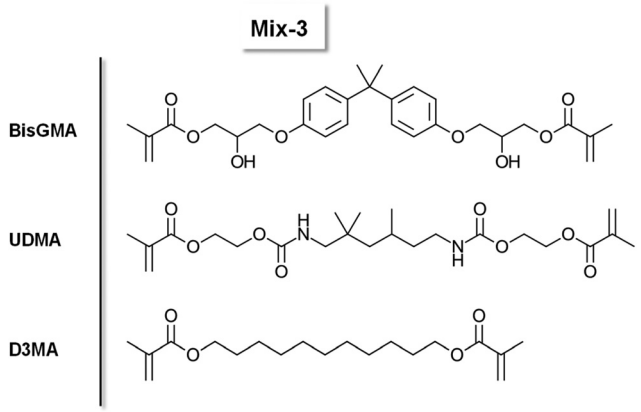

Scheme 2 Chemical structure of the monomers BisGMA, UDMA and D3MA. A mixture (4 : 4 : 2 (w%)) is referred to as Mix-3.

monomers composed of difunctional methacrylates with urethane and hydroxy moieties, (Mix-3, Scheme 2) commonly used in industrial applications, *e.g.* dental restoratives. This monomer mixture was chosen to stretch the robustness and effectivity of this new RPS and show the practicability that comes with this innovative approach. A systematical study of reactivity, chemical mechanism and polymer properties with respect to the newly developed RPS is presented in this work (Fig. 1).

Results and discussion

2K polymerizations applying different diboranes followed by rheology/IR and temperature measurements

The reactivity towards polymerization of a monomer is a crucial parameter to investigate for a new radical polymerization system (RPS). The following general study presents polymerization reactions of the monomer mixture Mix-3 (Scheme 2) initiated by the different diborane compounds (Scheme 1) after mixing with formulations containing the respective Cu compounds (Scheme 1) with regard to their polymerization reactivity.

The reactions were monitored *via* rheology/IR measurements. This specialized method setup allows for real-time characterization of mechanical properties (G') while simultaneously obtaining NIR data for the calculation of double bond conversion (DBC). In a first step, two respective formulations (Mix-3 + Diborane; Mix-3 + Cu compound) are homogenized for 45 s *via* rotational movement of the measuring stamp. Thereafter, the measurement starts and the storage modulus G' as well as loss modulus G'' of the mixed formulations is recorded. The intersection of G' and G'' is often seen as an indicator for the gel point,[34] however, in this work the time of steepest increase in storage modulus is referred to as gel time t_{gel} (ESI Fig. 3†). The redefinition of t_{gel} was necessary, because with long measurement times a long (>150 s) parallel section of G' and G'' was observed in which the intersection occurs, leading to no reproducible values for t_{gel} (ESI Fig. 4†). Following these changes, highly reproducible results were obtained for rheology measurements in this work. Simultaneously to the rheological measurement, NIR spectra of the polymerizing formulation were recorded with focus on the absorption band of the methacrylic double bond (~1640 cm^{-1}), leading to the calculation of the DBC (Fig. 2A).

In this work, the amount of diborane (shown in Scheme 1) and Cu complex (selected from Scheme 1) is always given with respect to the methacrylic double bond. For evaluation of the diboranes, unless otherwise stated, 3.5 mol% diborane and 0.2 mol% Cu(II)$(acac)_2$ were used.

Looking at the results, the six-membered ring diboranes (B6-1, B6-2, B63; Fig. 2C) show the effect of the steric demand in proximity to the boron–boron bond onto the reactivity towards initiation and further polymerization of the monomers. This steric effect is reflected in the t_{gel} of the formulations as more hindered B6-3 (and also sterically demanding B5-1) with four methyl groups do not lead to polymerization within 35 min. On the other hand, B6-1 and B6-2 were able to initiate the polymerization and exhibited t_{gel} < 17 min and <34 min respectively (Table 1). Here, B6-2 with two methyl groups in *ortho* position to the boron is more hindered in the availability of the B–B bond cleavage than B6-1 with two methyl groups in *para* position to the boron. Electronic effects of the substituents were not considered to be substantial and impactful for the radical reactivity, as it was assumed to be the same for B6-1, B6-2 and B6-3.

The five-membered B5-2 and B5-3 are asymmetrical compounds based on the pinacolatoboron moiety. In the case of B5-2 the additional 8-membered ring bearing the amine group leads to a donation of electrons into the B–B bond, weakening it and therefore making it more reactive towards cleavage catalyzed by the copper salt.[30] Furthermore, the donating effect may also lead to more reactive radicals, resulting in a faster initiation process. B5-3 is a silyl borane compound, described in literature to be more reactive than diboranes.[35,36] Looking at the results, this shows well in the observed reactivity towards polymerization as B5-3 exhibits the highest DBC with 57%. B5-2 exhibits high DBC (54%) and a fast t_{gel} (13.4 min) while showing even higher final G' than B5-3 (540 kPa compared to 500 kPa). These properties are attributed to a homogeneously formed network during the polymerization.

Furthermore, the polymerization of Mix-3 was monitored *via* the measurement of temperature during the polymerization reaction at room temperature and ambient atmosphere, giving a detailed insight into the polymerization kinetics (Fig. 2B). The sample size is much higher (>1 g) compared to rheology/IR measurements (200 mg), which allows for a greater influence of the Trommsdorff effect onto the polymerization. This is clearly seen in lower t_{max} (time of maximum temperature; estimation for gel time in polymerization temperature measurements) values compared to the respective t_{gel} which is only true in rheology/IR measurements. The highest peak temperature is reached using B5-2 as the diborane compound (T_{max} = 127.6 °C), highlighting the very reactive nature of this diborane initiator. The reactivity towards the polymeriz-

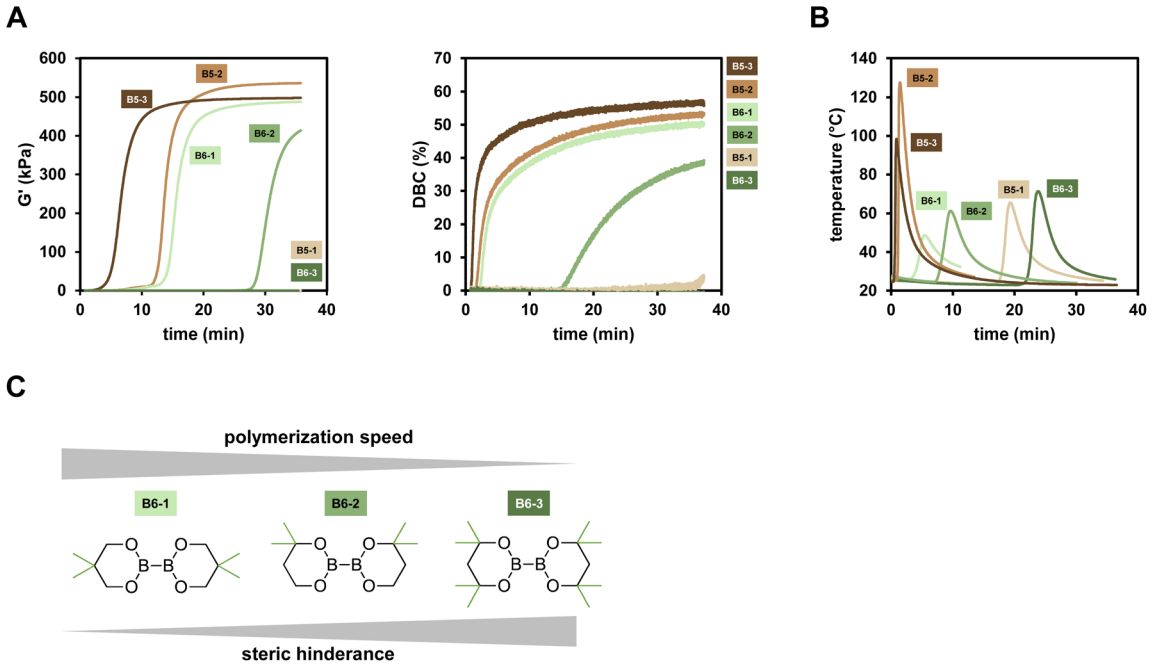

Fig. 2 (A) Rheology/IR measurements plotting G' and DBC as a function of the reaction time. 100 mg of formulations of Mix-3 containing 0.2 mol% Cu(II)(acac)$_2$ were mixed with 100 mg formulation of Mix-3 containing 3.5 mol% diborane. (B) Temperature measurements plotting the formulations temperature as a function of the reaction time. 0.9 g of formulations of Mix-3 containing 0.2 mol% Cu(II)(acac)$_2$ were mixed with 0.9 g formulation of Mix-3 containing 3.5 mol% diborane and the temperature was recorded. (C) Diborane compounds bearing a six-membered ring with increasing steric demand in proximity to the B–B bond, hence, resulting in lower polymerization speed with increased steric hinderance.

Table 1 Summarized data derived from rheology/IR measurements and temperature measurements of the polymerization of Mix-3 initiated by 0.2 mol% Cu(acac)$_2$ and 3.5 mol% of the respective diborane compound. Values for t_{gel}, G'_{end}, DBC$_{end}$, t_{max} and T_{max} are given. Cells marked with "–" could not be evaluated

	Rheology/IR			Temperature measurements	
	t_{gel} (min)	G'_{end} (kPa)	DBC$_{end}$ (%)	t_{max} (min)	T_{max} (°C)
B6-1	15.1	488	51.0	5.4	48.7
B6-2	29.6	414	39.3	9.7	61.3
B6-3	—	—	—	23.8	71.3
B5-1	—	—	—	19.3	65.4
B5-2	13.4	536	53.8	1.4	127.6
B5-3	6.3	498	57.4	0.9	98.4

ation of Mix-3 is in very good agreement to the rheology/IR measurements. Here, we could show that also the very hindered B5-1 and B6-3 lead to a polymerization in up to 15 min. The effect of steric hinderance in proximity to the B–B bond is well reflected in the observed data, since t_{max} is increasing from B6-1 to B6-2 to B6-3. Applying these compounds, curing times between <1 min and >15 min are achievable.

2K polymerizations applying different Cu compounds followed by rheology/IR and temperature measurements

The influence of the nature of the copper catalyst on the polymerization rate were subsequently investigated in detail. Herein, differently substituted Cu compounds with acetate (Cu(I)ac, Cu(II)ac$_2$), acetylacetonate (Cu(II)acac$_2$) and tri/hexa-fluorinated acetylacetonate (Cu(II)tfacac$_2$, Cu(II)hfacac)$_2$ ligands were investigated (Scheme 1). Based on the study in the previous chapter, B6-1 was chosen as ideal diborane compound to allow the proper investigation of positive as well as negative effects of the copper ligands on reactivity. Rheology/IR was used to determine DBC and gel time and polymerization temperature measurements were conducted, investigating the polymerization kinetics in a larger scale.

The results clearly showed that the nature of the ligand has a strong effect on the reactivity (Fig. 3A). Hence, the replacement of Cu(II)(acac)$_2$ with either Cu(I)acetate or Cu(II)(hfacac)$_2$ led to a significant acceleration of the polymerization reaction from around 15 min to <10 min (Table 2). Also Cu(II)(ac)$_2$ decreases t_{gel} making it more reactive than Cu(II)(acac)$_2$ and Cu(II)(tfacac)$_2$. It is argued that smaller ligands make the central copper atom more accessible towards the reaction with the respective diborane and therefore lead to an increase in reactivity. However, since Cu(II)(hfacac)$_2$ does not bear small ligand by any means, the improved solubility through substitution with six fluor atoms can increase the diffusion in the bulk monomer, leading to a higher probability of reacting with the diborane. Interestingly, Cu(II)(hfacac)$_2$ does not lead to high DBC throughout the reaction, ending with 36%, compared to over 50% achieved by Cu(II)(tfacac)$_2$, Cu(II)(ac)$_2$ and Cu(II)(acac)$_2$. The (hfacac)$_2$ ligated compound shows the highest polymerization temperature T_{max} as well as the fastest

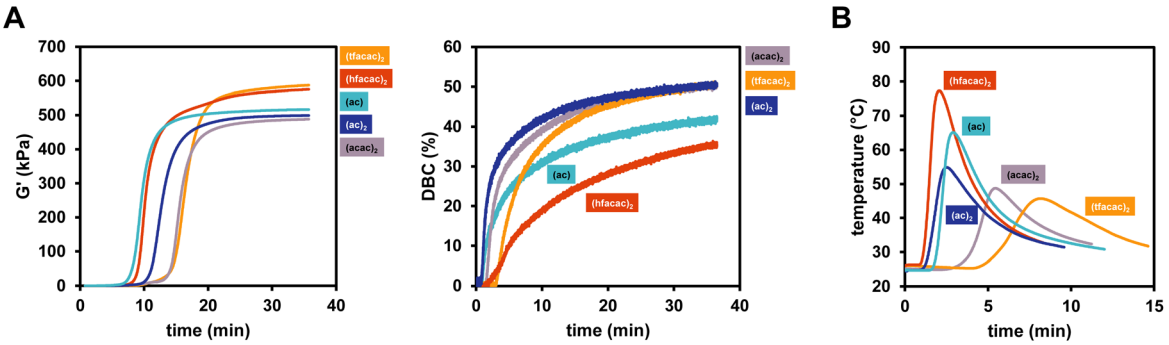

Fig. 3 (A) Rheology/IR measurements plotting G' and DBC as a function of the reaction time. 100 mg of formulations of Mix-3 containing 0.2 mol% copper salt were mixed with 100 mg formulation of Mix-3 containing 3.5 mol% B6-1. (B) Temperature measurements plotting the formulations temperature as a function of the reaction time. 0.9 g of formulations of Mix-3 containing 0.2 mol% copper salt were mixed with 0.9 g formulation of Mix-3 containing 3.5 mol% B6-1 and the temperature was recorded.

Table 2 Summarized data derived from rheology/IR measurements and temperature measurements of the polymerization of Mix-3 initiated by 0.2 mol% copper salt and 3.5 mol% B6-1. Values for t_{gel}, G'_{end}, DBC_{end}, t_{max} and T_{max} are given

	Rheology/IR			Temperature measurements	
	t_{gel} (min)	G'_{end} (kPa)	DBC_{end} (%)	t_{max} (min)	T_{max} (°C)
Cu(II)(acac)$_2$	15.1	488	51.0	5.4	48.7
Cu(II)(tfacac)$_2$	15.9	587	51.2	8.1	45.7
Cu(II)(hfacac)$_2$	9.8	575	36.3	2.1	77.3
Cu(II)(ac)$_2$	12.2	499	50.4	2.5	54.9
Cu(I)(ac)	9.2	516	42.6	2.9	65.1

polymerization, indicated by the lowest t_{max} (Fig. 3B). Remarkably, (acac)$_2$ and (tfacac)$_2$ lead to very high DBC over 50% and also very controllable curing times of around 15 min. Based on these results, Cu(II)(acac)$_2$ proved to be the ideal catalyst for further studies.

Effect of radical polymerization system concentration on initiating efficiency

To evaluate the limits and perspectives of this new initiating system for radical polymerization, different concentrations of diborane (B6-1) and Cu(II)(acac)$_2$ were used in this study, evaluating the polymerization reaction *via* rheology/IR measurements. The diborane concentration was varied between 0.5 mol% and 3.5 mol% while the Cu(II)(acac)$_2$ concentration was varied between 0.05 mol% and 0.2 mol%.

For both parts of the initiation system (diborane and Cu complex) it was shown that lower concentrations lead to a loss in initiation reactivity (Fig. 4A and B). This is reflected in a higher t_{gel} as well as lower G'_{end}. The progression of the DBC during the polymerization clearly corresponds to these results as the polymerization starts later and ends with lower DBC_{end} with lower concentrations. However, it is remarkable that even catalytic amounts of Cu(II)(acac)$_2$ (0.05 mol%) lead to a polymerization reaction with a DBC_{end} of over 30%. The diborane/Cu initiation system really shows its possibilities in initiation efficiency in this study as the reactivity can be tuned precisely *via* the concentration of the diborane or the Cu compound.

Chemical mechanism

Based on our novel approach, we have followed the initiating steps of the polymerization to establish mechanistic details. Accordingly, we have carried out experiments using spin-trap EPR, cyclovoltammetry (CV), and optical spectroscopy. The initiator combination of B6-1 and Cu(acac)$_2$ was chosen because it showed convenient curing times. First, the influence of the pH value and the addition of a radical scavenger should be evaluated by adding acetic acid, pyridine or TEMPO equimolar to the diborane initiator respectively.

We found that basic and acidic conditions do not have a highly significant influence on the polymerization of Mix-3 (Fig. 5A). On the other hand, in the presence of TEMPO as a radical scavenger, no polymerization was observed (green traces Fig. 5A). These results strongly support a radical propagation mechanism.

Accordingly, we have performed EPR experiments using 5,5-dimethyl-1-pyrroline-*N*-oxide (DMPO) as the spin-trapping agent (the use of *N*-*tert*-butyl-α-phenylnitrone (PBN) did not yield EPR spectra). The corresponding EPR spectra using B5-1 are shown in Fig. 5B (see the ESI† for control experiments). The simulation reveals a DMPO-derived radical with the hyperfine data, a(N) = 1.39 mT and a(H) = 1.22 mT. Highly related EPR spectra were observed with other diborane/Cu(II)(ac)$_2$ or Cu(II)(acac)$_2$ combinations. The lack of reference data does not allow us to unambiguously identify the trapped radicals but the hyperfine coupling constants point to B-type radical (Fig. 6).

These observations point to the formation of boron radicals *via* a redox reaction between the diborane and the copper salt. Accordingly, CV measurements were performed with B5-1. The corresponding cyclovoltammograms show no distinct oxidation wave in the region between 0 V and 1.4 V *vs.* Fc/Fc$^+$. Following the findings of Aelterman *et al.*,[37,38] we have per-

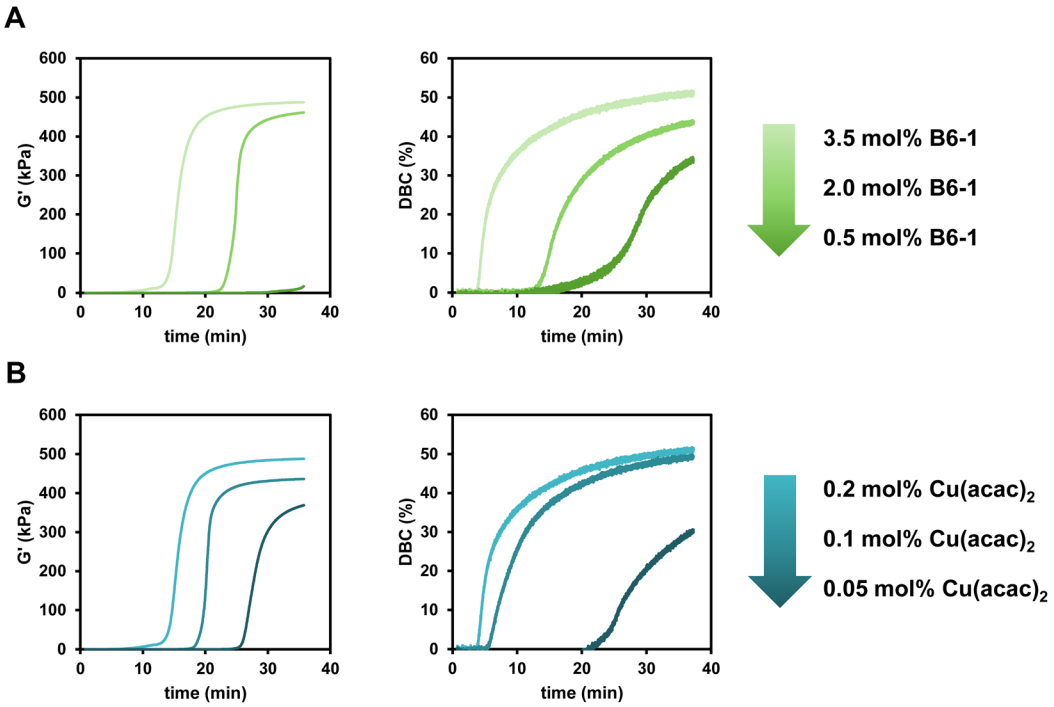

Fig. 4 (A) Rheology/IR measurements plotting *G'* and DBC as a function of the reaction time. 100 mg of formulations of Mix-3 containing 0.2 mol% copper salt were mixed with 100 mg formulation of Mix-3 containing 3.5 mol% (light green), 2.0 mol% (green) or 0.5 mol% (dark green) B6-1. (B) Rheology/IR measurements plotting *G'* and DBC as a function of the reaction time. 100 mg of formulations of Mix-3 containing 0.2 mol% (light blue), 0.1 mol% (blue) or 0.05 mol% (dark blue) copper salt were mixed with 100 mg formulation of Mix-3 containing 3.5 mol% B6-1.

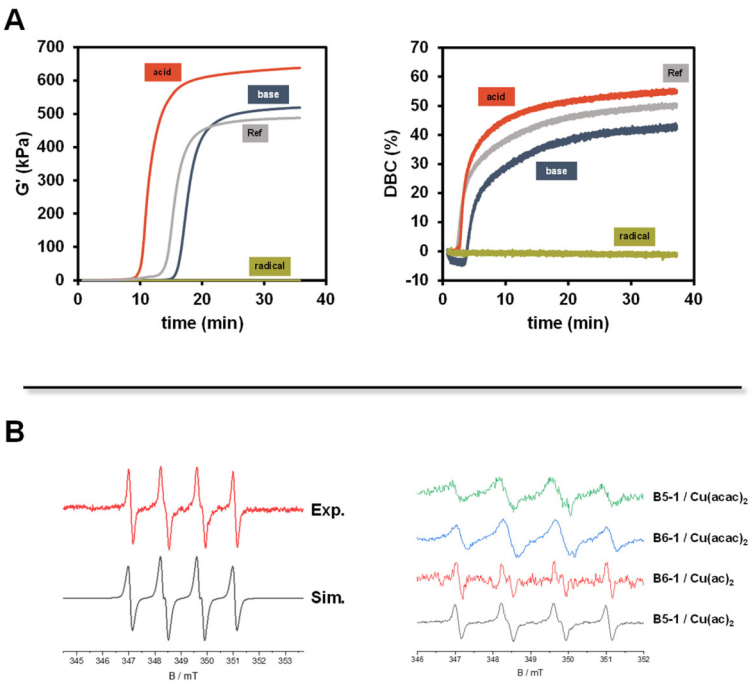

Fig. 5 (A) Rheology/IR measurements plotting *G'* and DBC as a function of the reaction time. 100 mg of formulations of Mix-3 containing 0.2 mol% copper salt were mixed with 100 mg formulation of Mix-3 containing 3.5 mol% B6-1 and 3.5 mol% of either acetic acid, pyridine or TEMPO. (B) Left: ESR-ST measurement of B5-1 and $Cu(ac)_2$ showing the formation of boryl radicals and the simulated spectra. (a(N) = 1.39 mT; a(H) = 1.22 mT; g = 2.0069). Right: ESR-ST measurements of B5-1 and B6-1 with $Cu(acac)_2$ and $Cu(ac)_2$ that all show the formation of boryl radicals.

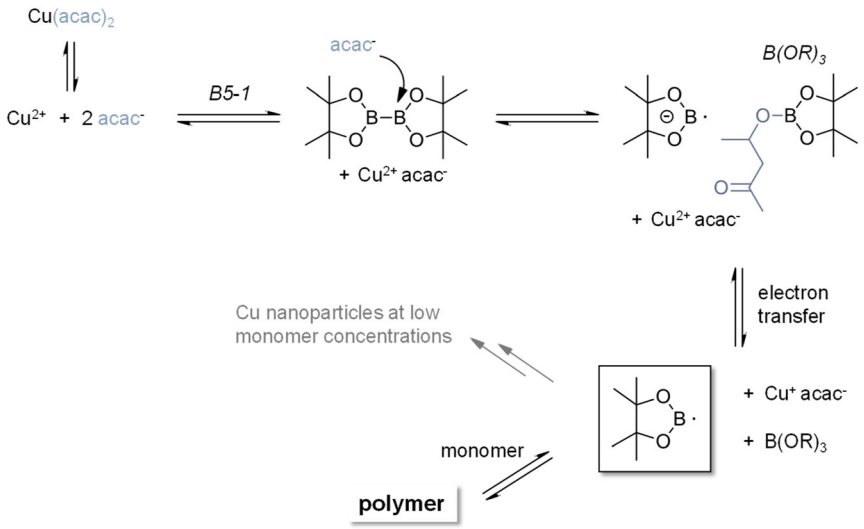

Fig. 6 Proposed mechanism for the initiation reaction between copper salt and diborane that yields the starting boryl radicals.

formed CV scans of Na(I)(acac) in the presence B5-1. Here the irreversible oxidation peak of Na(I)(acac) undergoes gradual shifts depending on the time interval after the addition of B5-1 until reaching a stationary state (ESI Fig. 6–8†). This points to a gradual association between the diborane and the acac anion and is consistent with the observation that the lag times for the 2K polymerization depend on the counterion (Fig. 3B). Moreover, an equimolar mixture of B5-1 with Cu(II)$(acac)_2$ leads to the emergence of a new oxidation wave at 0.53 V *vs.* Fc/Fc^+ (ESI Fig. 8†) indicating a new (electroactive) species. ^{11}B-NMR spectra of solutions containing B5-1 and (low amounts) of Cu(II)$(ac)_2$ show a resonance at 22.4 ppm in addition to that at 30.5 ppm (parent B5-1) revealing a partial decomposition of B5-1 and the formation of a $B(OR)_3$-type species (ESI Fig. 9†).[39]

Performing the reaction of the diborane/Cu(II) initiating system in diluted acrylate solutions (ESI Fig. 10†) leads to the emergence of a UV-Vis band at 560 nm after 20 minutes. Such a band is attributable to a surface plasmon band of Cu(0) nanoparticles.[40] This band can be (partially) quenched by bubbling with O_2. In bulk polymerization, this phenomenon does not emerge pointing to the bi-functionality of boryl radicals, which either add to double bonds or act as reducing agents (Fig. 6).

The combination of the EPR, UV-Vis, NMR, and cyclovoltammetric results together with published mechanistic considerations[41,42] led to the mechanism, which we suggest in Fig. 6. It considers that anions or strong nucleophiles have been reported to add to the boron centers of diboranes and cause the cleavage of the B–B bond.[43–46] This is in line with the formation of $B(OR)_3$ species, which were observed by NMR. It has to be borne in mind that a rather subtle combination of equilibrium reactions contributes to the controlled release of (boron-based) radicals,[47] which initiate the 2K polymerization. In particular the dissociation of the parent Cu^{2+} salt together with the nucleophilicity of the anion very likely influence the formation of the boryl radical anion and radical.

Stability of formulations

The application of this new 2K FRP initiation system requires a sufficient stability of the respective compounds in the bulk monomer. As this work aims to focus on difunctional methacrylate resins with several additional functional moieties (hydroxy and urethane) the stability was investigated in Mix-3. To this end, the reactivity of the initiation system was investigated after weeks of storage in the monomers (ESI Fig. 11†). It was shown in previous works that similar Cu salts are stable in the monomers, therefore focus was lain on the stability of the formulations containing diboranes.[48] In this regard, B6-1 and B5-2 were examined. The stability was determined *via* rheology measurements, tracking the t_{gel} over the course of weeks, referring to as long-time reactivity. It was shown that high stability for at least two weeks of storage is given in Mix-3, which implies a sufficient storage time for applications (ESI Fig. 11A†). Even higher stabilities were achieved in monomer mixtures without and with less functional moieties (ESI Fig. 11B and C†). In pure D3MA the stability of B6-1 proved to be very good as no loss in reactivity was found for storage over four weeks. The same conclusion can be drawn for B5-2 in a D3MA/BisGMA mixture. It occurred to us that the urethane moiety of UDMA leads to an interference with the RPS resulting in a loss of reactivity after 4 weeks, since we could observe a higher stability of formulations in monomer mixtures where UDMA was not present. This might be due to an unwanted premature cleavage of the diborane compound or due to an interaction of UDMA with the copper catalyst.

Polymer properties

The compounded polymers applying the new diborane/Cu initiation system in difunctional methacrylate monomer mixture Mix-3 were investigated regarding their mechanical properties. To this end, tensile test evaluating the stress and strain at break as well as $\Delta\sigma/\Delta\varepsilon$ were performed. Investigation

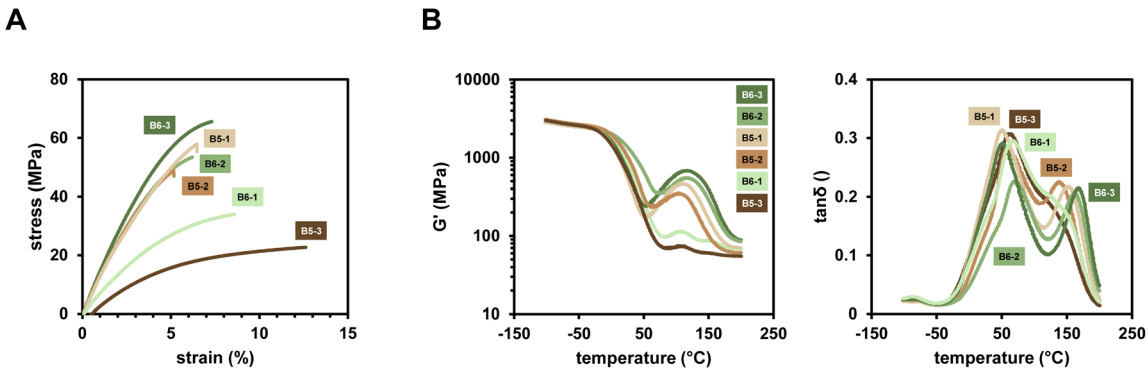

Fig. 7 (A) Stress/strain diagram derived from tensile tests of polymer samples using Mix-3 containing 0.2 mol% Cu(acac)$_2$ and 3.5 mol% diborane. (B) DMTA measurements depicting the storage modulus G' and the loss factor tan(δ) as a function of temperature (−100–200 °C). Samples were prepared from Mix-3 containing 0.2 mol% Cu(acac)$_2$ and 3.5 mol% diborane.

of thermal properties of the polymers, carried out *via* dynamic mechanical thermal analysis (DMTA) led to insights into T_g's and temperature dependency of G'. Polymers resulting from initiation *via* the investigated diboranes (Scheme 1) and Cu(II)(acac)$_2$ as well as B6-1 and the investigated Cu salts (Scheme 1) were examined in this study.

It was found that depending on which diborane compound is used, different properties can be achieved. Very flexible materials with high elongation at break and low T_g can be obtained by using *e.g.* B5-3 (Fig. 7A). On the other hand, highly robust materials with higher stress at break and high T_g are obtained when B6-3 is applied. Remarkably, the mechanical properties do not reflect the observed DBC measured with ATR-IR in the expected way (Table 3). B6-1, B6-2 and B6-3 lead to a very similar DBC, but the polymers show completely different mechanical behavior. Clearly, highly reactive initiation systems, such as B6-1 and B5-3, tend to form flexible networks. Considering a fast polymerization reaction, the gel point is reached with low number of crosslinks, leading to a soft network. The materials with the highest stress at break are formed by the least reactive diborane initiators B6-3 and B5-1. They lead to a slow formation of radicals, causing a very dense and more homogeneous network to form that has tougher mechanical properties. A whole variety of properties are achieved by using just different diboranes as the initiator for the polymerization. Additionally, almost no discoloration of the yielded polymer materials was observed since the diborane compounds are exclusively white solids and the colored copper salts are used in very low concentrations only. Furthermore, the specimens were color stable under air and showed no discoloration after weeks of storage (ESI Fig. 12†).

The DMTA measurements reveal, that in the case of the tougher materials, using B6-2, B6-3, B5-1 and B5-2, a post-curing process occurs above 50 °C (Fig. 7B). The storage modulus G' is increasing with increasing temperature, until the T_g of the newly formed post-cured network is reached at around 150 °C. In this regard, it was shown *via* differential scanning calorimetry (DSC) that thermal polymerization of Mix-3 is possible by using just the diborane initiator without copper salt (ESI Fig. 13†). The respective temperatures at which thermal polymerization starts for each diborane correspond to the post-curing temperatures of the polymer networks investigated in the DMTA measurements. This suggests a thermal initiation of diborane that is trapped inside the cured network, leading to the formation of new radicals in a network that is already soft and above the T_g. These radicals are readily used to form more crosslinks and a very homogeneous and densely crosslinked network is obtained.

Furthermore, DMTA measurements of a sample that was previously post-cured at 110 °C for 12 h confirmed that the network with T_g at 50 °C is completely replaced by the post-cured network with T_g > 150 °C (ESI Fig. 14†). Furthermore, these post-cured networks appear to be highly homogeneous. Compared to commercial FRP polymerized Mix-3,[50] the high T_g of the network is remarkable as well as the very narrow glass transition that confirms highly ordered network structures that can lead to superior mechanical properties[4] (ESI Fig. 15†).

In addition, mechanical properties of polymers derived from using various Cu(II) and Cu(I) ligands and B6-1 were investigated. Interestingly, the choice of ligand for the Cu complex leads to a severe difference in mechanical- as well as thermomechanical properties.

To this end, the slowly reacting Cu salts bearing the (acac)$_2$ and (tfacac)$_2$ ligand lead to the stiffest polymer networks

Table 3 Summarized data of mechanical and thermomechanical tests using polymer samples derived from Mix-3 containing 0.2 mol% Cu(acac)$_2$ and 3.5 mol% diborane

	Stress at break (MPa)	Elongation at break (%)	$\Delta\sigma/\Delta\varepsilon$ (MPa)	$DBC_{ATR\text{-}IR}$ (%)
B6-1	27.6 ± 4.1	6.0 ± 1.6	7.6	80
B6-2	49.8 ± 3.2	5.7 ± 0.5	13.7	72
B6-3	64.1 ± 2.1	7.2 ± 0.9	15.2	79
B5-1	55.1 ± 3.2	6.4 ± 0.4	13.9	>80
B5-2	47.9 ± 0.7	4.8 ± 0.3	13.5	58
B5-3	17.6 ± 4.9	7.7 ± 3.1	5.1	46

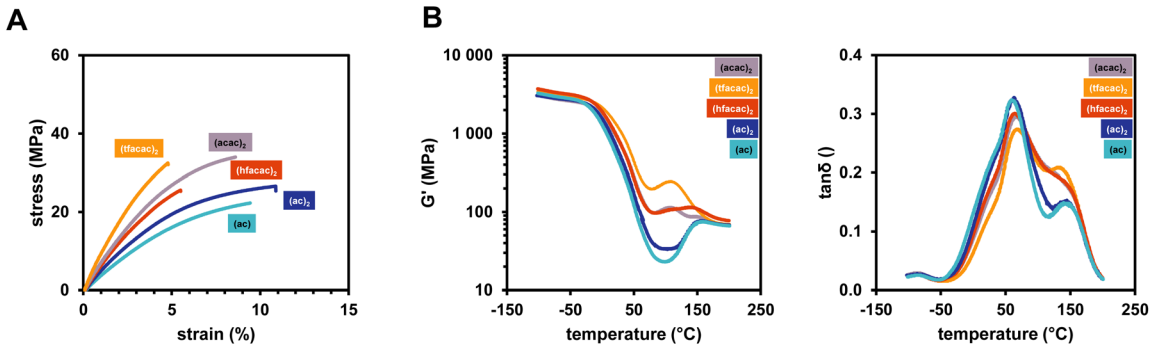

Fig. 8 (A) Stress/strain diagram derived from tensile tests of polymer samples using Mix-3 containing 0.2 mol% copper salt and 3.5 mol% B6-1. (B) DMTA measurements depicting the storage modulus G' and the loss factor tan(δ) as a function of temperature (–100–200 °C). Samples were prepared from Mix-3 containing 0.2 mol% copper salt and 3.5 mol% B6-1.

Table 4 Summarized data of mechanical and thermomechanical tests using polymer samples derived from Mix-3 containing 0.2 mol% copper salt and 3.5 mol% B6-1

	Stress at break (MPa)	Elongation at break (%)	$\Delta\sigma/\Delta\varepsilon$ (MPa)	$DBC_{ATR\text{-}IR}$ (%)
Cu(II)(acac)$_2$	27.6 ± 4.1	6 ± 1.6	7.6	79
Cu(II)(tfacac)$_2$	27.1 ± 7.1	5.3 ± 1.2	10.0	84
Cu(II)(hfacac)$_2$	22.4 ± 3	4.8 ± 1.1	7.0	70
Cu(II)(ac)$_2$	22.9 ± 2.8	9 ± 1.4	5.7	63
Cu(I)(ac)	19.3 ± 2.2	8.6 ± 2.2	4.4	44

(Fig. 8A). This is again attributed to a slow network formation and therefore the development of a more homogeneous network structure. The very reactive Cu complexes (Cu(II)(hfacac)$_2$, Cu(II)(ac)$_2$, Cu(I)(ac)) lead to a very fast gelation and a less crosslinked network, having more elastic properties with high elongation at break (>10%) (Table 4). The faster gelation and less crosslinks perfectly correspond to the lower DBC that was obtained from ATR-IR measurements. The progression of G' during the DMTA measurements also highlights these properties as for the softer networks there is really only one T_g and very little post-curing at higher temperatures over 100 °C (Fig. 8B). The stiffer networks (especially (acac)$_2$) already lead to post-curing at around 50 °C. The choice of the copper ligand offers the possibility to tune the material properties by introducing different solubilities and accessibilities for reaction with the diborane. However, the acetylacetonate ligands proved to lead to superior properties compared to the acetates, also referring to the higher DBC.

Conclusion

A radical polymerization system (RPS) based on a diborane compound and a copper complex was introduced as a powerful and versatile tool for 2K polymerization of methacrylate monomers without the use of amines and peroxides. We were able to prove a radical initiation as well as a radical propagation mechanism for this new RPS. Furthermore, we found that the reactivity towards initiation of free radical polymerization is highly dependent on steric influences in proximity to the boron–boron bond. To this end, sterically hindered diboranes proved to lead to longer working times >20 min and less hindered diboranes showed polymerization after 5 min. One diborane compound (B5-2) was particularly promising, as intramolecular activation of the boron–boron bond led to high reactivity despite being sterically demanding. Additionally, we could show that the reactivity can not only be tuned by the choice of the diborane but also by the copper ligand. Since high stability was given in diverse combinations of methacrylic monomers, thermomechanical- and mechanical properties of polymer networks obtained by employing the new diborane/Cu RPS were characterized. We could show significant influence of the RPS on the final properties of the polymers and were able to obtain very promising mechanical strength of highly homogeneous polymer networks. Furthermore, the polymerization speed would influence the mechanical properties of the polymer network due to differences in the network density that may be caused by termination reactions of very fast reacting systems leading to a shorter kinetic chain length and therefore more homogeneous and softer networks. To conclude, the use of the diborane/Cu RPS has proven to have very high potential in introducing a new 2K initiation system that comes without the use of toxic amines and thermally unstable peroxides and shows high reactivity, good stability and can lead to homogeneous polymer networks with excellent mechanical strength.

Experimental part

Synthesis of bis(3-methylbutane-1,3-diol)diborane (B6-2)

A solution of $B_2(NMe_2)_4$ (1 eq., 4.64 mmol) in dry Et_2O (20 mL) was prepared inside a glovebox. 3-Methylbutane-1,3-diol (2.22 eq., 10.3 mmol) in 20 mL dry Et_2O were added under argon atmosphere. The reaction mixture was stirred at room temperature for 12 h. Thereafter, a 1 M solution of HCl in Et_2O (4 eq.) was added and the mixture was stirred for another 6 h at room temperature. The reaction mixture was filtered and all

volatiles were removed *in vacuo*. The product was recrystallized from *n*-hexane to yield white solid needles (m.p. 62.3 °C).[49] ^{11}B NMR (128 MHz, Chloroform-d) δ 27.87. ^{1}H NMR (200 MHz, Chloroform-d) δ 4.06–3.93 (m, 1H), 1.85–1.72 (m, 1H), 1.31 (s, 3H) (ESI Fig. 1 and Fig. 2†).

NMR

NMR spectra were recorded on a Bruker DPX-200 FT-NMR spectrometer at 200 MHz for ^{1}H and 50 MHz for ^{13}C, as well as on a Bruker Avance DRX-400 FT-NMR spectrometer at 400 MHz for ^{1}H and 100 MHz for ^{13}C. The signals are recorded according to their chemical shifts, which were reported in ppm (s = singlet, d = doublet, t = triplet, q = quartet, qn = quintet, sep = septet, m = multiplet, bs = brad singlet) in comparison to tetramethylsilane (d = 0 ppm). The spectra were then referenced on the used NMR-solvent [^{1}H: $CDCl_3$ (7.26 ppm), ^{13}C: $CDCl_3$ (77.16 ppm)].

Rheology/IR measurements

Rheology measurements were performed with a real time-near infrared rheometer consisting of an Anton Paar MCR 302 WESP with a P-PTD 200/GL Peltier glass plate and a PP25 measuring system coupled with a Bruker Vertex 80 FTIR spectrometer with an MCT detector. 100 mg of each respective 2K-formulation was placed at the center of the glass plate, which was covered with a PE tape and the measurements were conducted at 25 °C with an Anton Paar H-PTD 200 furnace and a gap of 200 µm. The rheology stamp was rotated for 45 s to ensure homogeneous mixture of the 2K formulations. The polymerizing sample was sheered with a strain of 1% and a frequency of 1 Hz. The NIR-spectra were evaluated using OPUS 7.0 software, integrating the signals at a wavelength of ~6140 cm^{-1}. DBC was determined as the ratio of peak areas at the start and each respective time during the measurement.

Polymerization temperature measurements

For temperature measurements, 0.9 g of each of the respective 2K formulations were weighed out and mixed in a silicon mold (15 × 15 × 15 mm) under air at room temperature. During the curing of the formulation the temperature was measured with a RS thermocouple type "K" submerged into the formulation and processed with a Picolog 6.2.6.

ESR-ST

Stock solutions of the copper salts and the boron compounds in acetonitrile are prepared. The stock solutions were combined with a spin trap (DMPO; 5,5-dimethyl-1-pyrrolin-*N*-oxide). The final concentrations were: 0.57 mM Cu-salt, 10 mM boron compound and 50 mM spin trap. The mixture is filled into a capillary and EPR spectra are recorded on a Bruker EMX spectrometer. For simulations the WinSIM software was used.

Cyclovoltammetry

Cyclovoltammetric measurements were conducted under argon with a Pt disc working electrode, a Pt wire counter-electrode and an Ag pseudo-reference electrode. Potentials were referenced onto the Fc/Fc^{+} standard and are reported *versus* the standard hydrogen electrode. For all measurements the used solvent was a dry 0.1 M solution of tBu$_4$NClO$_4$ in dimethylformamide. The scan rate was 300 mV s^{-1} for all measurements.

DMTA

For the DMTA measurements, polymer specimens were fabricated in a silicone mold (sticks, 5 × 2 × 40 mm). Subsequently, the specimens were post-cured for 24 h at 37 °C. Thereafter, the specimens were sanded until uniform dimensions (<±0.1 mm) were reached. DMTA measurements were performed with an Anton Paar MCR 301 with a CTD 450 oven and an SRF 12 measuring system. Polymer specimens were tested in torsion mode with a frequency of 1 Hz and strain of 0.1%. The temperature was increased from −100 °C to 200 °C with a heating rate of 2 °C min^{-1}. The storage modulus and the loss factor of the polymer samples was recorded with the software Rheoplus/32 V3.40 from Anton Paar.

Tensile tests

Tensile test specimens were prepared in accordance to DMTA specimen. The dog chew bone-shaped samples met the requirements for ISO 527 test specimen 5b (total length of 35 mm and a parallel region dimension of 2 × 2 × 12 mm). Five specimens were tested per sample. The tests themselves were performed on a Zwick Z050 with a maximum test force of 50 kN. The specimens were fixed between two clamps and strained with a traverse speed of 5 mm min^{-1}. A stress/strain plot was recorded simultaneously.

Data availability

The data that support the findings of this study are available from the corresponding author, Patrick Knaack, upon reasonable request.

Author contributions

Florian Pieringer: data curation, formal analysis, investigation, methodology, visualization, writing – original draft, writing – review & editing; Konstantin Knaipp: data curation, formal analysis, investigation; Robert Liska: conceptualization, supervision, project administration; Yohann Catel: conceptualization, supervision, project administration; Norbert Moszner: conceptualization, supervision, project administration; Georg Gescheidt: conceptualization, supervision, project administration, writing – original draft; Patrick Knaack: conceptualization, supervision, project administration.

Conflicts of interest

The authors declare no competing financial interest.

References

1 P. Garra, C. Dietlin, F. Morlet-Savary, F. Dumur, D. Gigmes, J.-P. Fouassier and J. Lalevée, Redox two-component initiated free radical and cationic polymerizations: Concepts, reactions and applications, *Prog. Polym. Sci.*, 2019, **94**, 33–56.

2 R. A. Guggenberger, R. Hecht, M. Ludsteck and G. Raia, Stippschild-Boxler Twocomponent self-adhesive dental composition, process of production and use thereof, US10932994B2, 2015.

3 Z. Y. Duymus, N. D. Yanikoğlu and M. Alkurt, Evaluation of the flexural strength of dual-cure composite resin cements, *J. Biomed. Mater. Res., Part B*, 2013, **101**, 878–881.

4 G. Peer, A. Eibel, C. Gorsche, Y. Catel, G. Gescheidt, N. Moszner and R. Liska, Ester-Activated Vinyl Ethers as Chain Transfer Agents in Radical Photopolymerization of Methacrylates, *Macromolecules*, 2019, **52**, 2691–2700.

5 S. C. Ligon, B. Husár, H. Wutzel, R. Holman and R. Liska, Strategies to Reduce Oxygen Inhibition in Photoinduced Polymerization, *Chem. Rev.*, 2014, **114**, 557–589.

6 C. Haslinger, L. P. Leutgeb, M. Haas, S. Baudis and R. Liska, Synthesis and Photochemical Investigation of Tetraacylgermanes, *ChemPhotoChem*, 2022, **6**, e202200108.

7 A. Arar, H. Mokbel, F. Dumur and J. Lalevée, High Performance Redox Initiating Systems Based on the Interaction of Silane with Metal Complexes: A Unique Platform for the Preparation of Composites, *Molecules*, 2020, **25**, 1602.

8 P. Garra, F. Morlet-Savary, B. Graff, F. Dumur, V. Monnier, C. Dietlin, D. Gigmes, J. P. Fouassier and J. Lalevée, Metal Acetylacetonate–Bidentate Ligand Interaction (MABLI) as highly efficient free radical generating systems for polymer synthesis, *Polym. Chem.*, 2018, **9**, 1371–1378.

9 A. Arar, A. A. Mousawi, C. Boyadjian, P. Garra, J. P. Fouassier and J. Lalevee, Diphenylsilane-Manganese Acetylacetonate Redox Initiating Systems: Toward Amine-Free and Peroxide-Free Systems, *Macromol. Chem. Phys.*, 2020, **221**, 2000058.

10 D. S. Achilias and I. Sideridou, Study of the Effect of two BPO/Amine Initiation Systems on the Free-Radical Polymerization of MMA used in Dental Resins and Bone Cements, *J. Macromol. Sci., Part A: Pure Appl.Chem.*, 2002, **39**, 1435–1450.

11 D. S. Achilias and I. D. Sideridou, Kinetics of the benzoyl peroxide/amine initiated free-radical polymerization of dental dimethacrylate monomers: Experimental studies and mathematical modeling for TEGDMA and Bis-EMA, *Macromolecules*, 2004, **37**, 4254–4265.

12 I. D. Sideridou, D. S. Achilias and O. Karava, Reactivity of Benzoyl Peroxide/Amine System as an Initiator for the Free Radical Polymerization of Dental and Orthopaedic Dimethacrylate Monomers: Effect of the Amine and Monomer Chemical Structure, *Macromolecules*, 2006, **39**, 2072–2080.

13 F. Falkensammer, G. V. Arnetzl, A. Wildburger and J. Freudenthaler, Color stability of different composite resin materials, *J. Prosthet. Dent.*, 2013, **109**, 378–383.

14 A. Falsafi, R. Kalgutkar and J. D. Oxman, Dental compositions and methods with arylsulfinate salts, US7465758B2, 2004.

15 R. Hecht and M. Ludsteck, Initiator system for acid dental formulations, US6953535B2, 2002.

16 M. Kawashima and I. Omura, Polymerizable Composition, EP0408357B1, 1990.

17 N. Moszner, T. Köhler, J. Schädlich and J. Angermann, Dental materials based on redox systems with low-odour cumene hydroperoxide derivatives, US2020/0253837A1, p. 2022.

18 G. Raia, R. Hecht, M. Ludsteck and J. D. Oxman, Polymerizable compositions containing salts of barbituric acid derivatives, p. US20090192239A1, 2007.

19 I. Yoji, K. Yoshinori and T. Kawashima, Polymerization initiator composition controlling polymerization at interface and curable composition containing same, US5166117A, 1991.

20 F. Pieringer, Y. Catel, R. Liska, N. Moszner and P. Knaack, Group transfer polymerization in bulk methacrylates, *J. Polym. Sci.*, 2023, **61**, 2922–2931.

21 D. Wang, P. Garra, F. Szillat, J. P. Fouassier and J. Lalevée, Silane Based Redox Initiating Systems: Toward a Safer Amine-Free, Peroxide-Free, and Metal-Free Approach, *Macromolecules*, 2019, **52**, 3351–3358.

22 P. Garra, F. Dumur, D. Gigmes, M. Nechab, F. Morlet-Savary, C. Dietlin, S. Gree, J. P. Fouassier and J. Lalevée, Metal Acetylacetonate–Bidentate Ligand Interaction (MABLI) (Photo)activated Polymerization: Toward High Performance Amine-Free, Peroxide-Free Redox Radical (Photo)initiating Systems, *Macromolecules*, 2018, **51**, 2706–2715.

23 M. Le Dot, N. Giacoletto, F. Morlet-Savary, B. Graff, V. Monnier, D. Gigmes, M. Nechab, F. Dumur, P. Gerard and J. Lalevée, Synergistic approach of type I hybrid complexes for highly efficient metal-based initiating strategies: Toward low energy-consuming polymerization for thermoplastic composite implementation, *Eur. Polym. J.*, 2023, **186**, 111871.

24 S. Mun, J.-E. Lee and J. Yun, Copper-catalyzed beta-Boration of alpha,beta-unsaturated carbonyl compounds: rate acceleration by alcohol additives, *Org. Lett.*, 2006, **8**, 4887–4889.

25 G. Wang, H. Zhang, J. Zhao, W. Li, J. Cao, C. Zhu and S. Li, Homolytic Cleavage of a B–B Bond by the Cooperative Catalysis of Two Lewis Bases: Computational Design and Experimental Verification, *Angew. Chem., Int. Ed.*, 2016, **55**, 5985–5989.

26 M. Eck, S. Würtemberger-Pietsch, A. Eichhorn, J. H. J. Berthel, R. Bertermann, U. S. D. Paul, H. Schneider, A. Friedrich, C. Kleeberg, U. Radius and T. B. Marder, B–B bond activation and NHC ring-expansion reactions of diboron(4) compounds, and accurate molecular structures

of B2(NMe2)4, B2eg2, B2neop2 and B2pin2, *Dalton Trans.*, 2017, **46**, 3661–3680.

27 T. Kou, I. Tatsuo and M. Norio, Addition and Coupling Reactions of Bis(pinacolato)diboron Mediated by CuCl in the Presence of Potassium Acetate, *Chem. Lett.*, 2000, **29**, 982–983.

28 H.-S. Sim, X. Feng and J. Yun, Copper-Catalyzed Enantioselective β-Boration of Acyclic Enones, *Chem. – Eur. J.*, 2009, **15**, 1939–1943.

29 J.-B. Xie, S. Lin, S. Qiao and G. Li, Asymmetric Catalytic Enantio- and Diastereoselective Boron Conjugate Addition Reactions of α-Functionalized α,β-Unsaturated Carbonyl Substrates, *Org. Lett.*, 2016, **18**, 3926–3929.

30 M. Gao, S. B. Thorpe, C. Kleeberg, C. Slebodnick, T. B. Marder and W. L. Santos, Structure and Reactivity of a Preactivated sp2–sp3 Diboron Reagent: Catalytic Regioselective Boration of α,β-Unsaturated Conjugated Compounds, *J. Org. Chem.*, 2011, **76**, 3997–4007.

31 A. J. J. Lennox and G. C. Lloyd-Jones, Selection of boron reagents for Suzuki–Miyaura coupling, *Chem. Soc. Rev.*, 2014, **43**, 412–443.

32 F. Mo, Y. Jiang, D. Qiu, Y. Zhang and J. Wang, Direct Conversion of Arylamines to Pinacol Boronates: A Metal-Free Borylation Process, *Angew. Chem., Int. Ed.*, 2010, **49**, 1846–1849.

33 N. Takemura, Y. Sumida and H. Ohmiya, Organic Photoredox-Catalyzed Silyl Radical Generation from Silylboronate, *ACS Catal.*, 2022, **12**, 7804–7810.

34 C. Gorsche, R. Harikrishna, S. Baudis, P. Knaack, B. Husar, J. Laeuger, H. Hoffmann and R. Liska, Real Time-NIR/MIR-Photorheology: A Versatile Tool for the in Situ Characterization of Photopolymerization Reactions, *Anal. Chem.*, 2017, **89**, 4958–4968.

35 M. Suginome and Y. Ito, Transition-Metal-Catalyzed Additions of Silicon–Silicon and Silicon–Heteroatom Bonds to Unsaturated Organic Molecules, *Chem. Rev.*, 2000, **100**, 3221–3256.

36 C. Kleeberg and C. Borner, On the Reactivity of Silylboranes toward Lewis Bases: Heterolytic B–Si Cleavage vs, Adduct Formation, *Eur. J. Inorg. Chem.*, 2013, **2013**, 2799–2806.

37 M. Aelterman, P. Jubault and T. Poisson, Electrochemical Borylation of Electron-Deficient Alkenes and Allenoates, *Eur. J. Org. Chem.*, 2023, **26**, e202300063.

38 M. Aelterman, M. Sayes, P. Jubault and T. Poisson, Electrochemical Hydroboration of Alkynes, *Chem. – Eur. J.*, 2021, **27**, 8277–8282.

39 H. Nöth and B. Wrackmeyer, in *Nuclear Magnetic Resonance Spectroscopy of Boron Compounds*, ed. P. Diehl, E. Fluck and R. Kosfeld, Springer Berlin, Heidelberg, 1978.

40 L.-S. Jhuang, G. Kumar and F.-C. Chen, Localized surface plasmon resonance of copper nanoparticles improves the performance of quasi-two-dimensional perovskite light-emitting diodes, *Dyes Pigm.*, 2021, **188**, 109204.

41 F. W. Friese and A. Studer, New avenues for C-B bond formation *via*, radical intermediates, *Chem. Sci.*, 2019, **10**, 8503–8518.

42 C. C. Guo, P. F. Li, S. Y. Wang, Y. W. Wang, N. Liu, Q. Q. Bu and Y. A. Qiu, Selective Electroreductive Hydroboration of Olefins with B_2pin_2, *J. Org. Chem.*, 2023, **88**, 4569–4580.

43 L. Kuehn, L. Zapf, L. Werner, M. Stang, S. Würtemberger-Pietsch, I. Krummenacher, H. Braunschweig, E. Lacôte, T. B. Marder and U. Radius, NHC induced radical formation *via* homolytic cleavage of B-B bonds and its role in organic reactions, *Chem. Sci.*, 2022, **13**, 8321–8333.

44 L. L. Liu and D. W. Stephan, Radicals derived from Lewis acid/base pairs, *Chem. Soc. Rev.*, 2019, **48**, 3454–3463.

45 H. T. Lu, Z. Y. Geng, J. Y. Li, D. P. Zou, Y. S. Wu and Y. J. Wu, Metal-Free Reduction of Aromatic Nitro Compounds to Aromatic Amines with B_2pin_2 in Isopropanol, *Org. Lett.*, 2016, **18**, 2774–2776.

46 X. Zhang, A. Friedrich and T. B. Marder, Copper-Catalyzed Borylation of Acyl Chlorides with an Alkoxy Diboron Reagent: A Facile Route to Acylboron Compounds, *Chem. – Eur. J.*, 2022, **28**, e202201329.

47 L. Zhang and L. Jiao, Super electron donors derived from diboron, *Chem. Sci.*, 2018, **9**, 2711–2722.

48 P. Garra, F. Dumur, M. Nechab, F. Morlet-Savary, C. Dietlin, B. Graff, D. Gigmes, J.-P. Fouassier and J. Lalevée, Stable copper acetylacetonate-based oxidizing agents in redox (NIR photoactivated) polymerization: an opportunity for the one pot grafting from approach and an example on a 3D printed object, *Polym. Chem.*, 2018, **9**, 2173–2182.

49 W. Clegg, T. R. F. Johann, T. B. Marder, N. C. Norman, A. Guy Orpen, T. M. Peakman, M. J. Quayle, C. R. Rice and A. J. Scott, Platinum-catalysed 1,4-diboration of 1,3-dienes, *J. Chem. Soc., Dalton Trans.*, 1998, 1431–1438.

50 V. A. Lopyrev, M. G. Voronkov, E. N. Baiborodina, N. S. Shaglayeva and T. N. Rakhmatulina, On the mechanism of initiation of polymerization by an oxidant–thiourea system, *J. Polym. Sci., Polym. Chem. Ed.*, 1979, **17**, 3411–3412.

